The Outer Edge of Saturn's B Ring

Joseph M. Hahn
Space Science Institute
Austin, TX

Joseph Spitale
CICLOPS/SSI
Tucson, AZ

Carolyn Porco
CICLOPS/SSI
Boulder, CO

Introduction

The outer edge of Saturn's main A ring is confined by $m = 7$ inner Lindblad resonances (ILRs) with the coorbital satellites Janus and Epimetheus, while the outer B ring is confined by an $m = 2$ ILR with the satellite Mimas (Porco et al 1984). The following outlines a detailed dynamical model of these interesting ring-satellite systems. This model accounts for the satellite's perturbations, as well as the ring's internal forces—ring self gravity, pressure, and viscosity, as well as the possible drag forces (e.g., plasma, Poynting-Robertson, and/or Yarkovsky drag) that might affect smaller ring particles, too. Our goal is to understand how the ring's response to the satellite's perturbations also depends on the ring's physical parameters: its unperturbed surface density σ_0, the ring particles' dispersion velocity c, the ring's viscosity ν, and strength of the drag force. Comparisons of the model to spacecraft observations of the ring-edges should then provide estimates of, or else limits on, the ring parameters σ, c, ν, and $C_{\rm drag}$.

Equations of motion

A ring particle's trajectory $\mathbf{r}(t)$ obeys Newton's second law of motion,

$$\ddot{\mathbf{r}} = -\nabla(\Phi_p + \Phi_s) + \mathbf{a} \qquad (1)$$

where Φ_p and Φ_s are the gravitational potentials of the central planet and satellite, and $\mathbf{a} = \mathbf{a}_g + \mathbf{a}_p + \mathbf{a}_\nu + \mathbf{a}_{\rm drag} = A_r\hat{\mathbf{r}} + A_\theta\hat{\theta}$ are the particle's accelerations due to ring gravity, pressure, viscosity, and the hypothetical drag force, with A_r and A_θ the total radial and tangential accelerations. A Fourier expansion of the perturbations then makes Eqn. (1) more manageable,

$$\Phi_s(\mathbf{r}) \simeq \phi_s^m(r)e^{im(\theta-\theta_s)} \qquad (2)$$
$$A_r(\mathbf{r}) \simeq A_r^0(r) + A_r^m(r)e^{im(\theta-\theta_s)} \qquad (3)$$
$$A_\theta(\mathbf{r}) \simeq A_\theta^0(r) + A_\theta^m(r)e^{im(\theta-\theta_s)}, \qquad (4)$$

remembering to preserve only the real parts of all equations. The ring's particle's response to perturbations is an epicyclic trajectory

$$r(t) = a - R_m e^{i(m\theta_0+\omega_m t - m\tilde{\omega})} \simeq a - R_m e^{im(\theta-\theta_s-\tilde{\omega})}, \qquad (5)$$

where a is the particle's semimajor axis, $R_m = ea$ is the particle's epicyclic amplitude, e its forced eccentricity, $\omega_m = m(\Omega - \Omega_s)$ is the satellite's forcing frequency where Ω and Ω_s are the particle's and satellite's angular velocities, and $\tilde{\omega}$ is the particle's longitude of periapse. Inserting Eqn. (5) into (1) and linearizing then provides the particle's epicyclic amplitude

$$R_m = -\frac{\Psi_s^m - 2i\varepsilon A_\theta^m + A_r^m}{D}e^{im\tilde{\omega}}, \qquad (6)$$

where $D = \kappa^2 - \Omega_m^2$ is the particle's frequency-distance from resonance, $\kappa \simeq \Omega$ is the epicyclic frequency, and $\Psi_s^m = -\partial\phi_s^m/\partial a - 2\varepsilon m\phi_s^m/a$ is the satellite's forcing function. A Lindblad resonance (LR) is a site where $D(a) = 0$ or $\kappa = \varepsilon\omega_m$, with $\varepsilon = +1$ at an inner LR and $\varepsilon = -1$ at an outer LR.

streamlines: Eqn. (6) requires the $m^{\rm th}$ Fourier components of the ring's radial and tangential accelerations, A_r^m and A_θ^m. Their calculation is greatly simplified by the concept of *streamlines* (Borderies et al 1985), which are the trajectories traced by the right-hand side of Eqn. (5). A broad planetary ring is then regarded as the sum of many streamlines whose eccentricities $e(a)$ and longitudes of periapse $\tilde{\omega}(a)$ are functions of semimajor axes a.

Simple mass conservation relates the the ring's surface density to the streamlines' orbit elements via

$$\sigma(a,\theta) = \frac{\sigma_0(a)}{J}, \quad J(a,\theta) = \frac{\partial r}{\partial a} \simeq 1 - q\cos[m(\theta-\theta_s-\tilde{\omega})], \quad q \simeq \left|\frac{\partial(ae)}{\partial a}\right| \qquad (7)$$

where J^{-1} is the ring's compression and q is the nonlinearity parameter of Borderies et al (1985). The following analysis also makes the *local approximation*, which assumes that the ring's force on a particle is exerted by nearby streamlines that resemble long, straight wires of matter.

ring self gravity: In the local approximation, the gravitational acceleration that a streamline exerts on a ring particle is $\delta a_g = 2G\lambda/d$, where $\lambda = \sigma_0(a')\delta a'$ is the streamline's linear mass density, $\delta a'$ is the streamline's semimajor axis width, and $d = r' - r$ is the particle's distance from the perturbing streamline. The acceleration that the entire ring exerts on a particle is

$$a_g = \int_{\rm ring}\delta a_g = \int_{a_{\rm in}}^{a_{\rm out}}\frac{2G\sigma_0(a')da'}{r(a',\theta) - r(a,\theta)} \simeq A_{gr}^0 + A_{gr}^m e^{im(\theta-\theta_s)} \qquad (8)$$

where the A_{gr}^m are the $m^{\rm th}$ Fourier components of the ring's gravitational acceleration that are function of the ring's orbit elements $e(a)$ and $\tilde{\omega}(a)$ and surface density $\sigma_0(a)$. Formulas for the A_r^m and A_θ^m are all too ponderous for this presentation, but are instead detailed in Hahn et al (2008).

ring pressure: Collisions among ring particle also result in an acceleration due to pressure that, in the hydrodynamic approximation, is

$$a_p = -\frac{c^2}{\sigma}\frac{\partial\sigma}{\partial r} \simeq A_{pr}^0 + A_{pr}^m e^{im(\theta-\theta_s)} \qquad (9)$$

where c is the ring particles' dispersion velocity. The Fourier coefficients for this acceleration, A_{pr}^m, are again complicated functions of the $e(a)$, $\tilde{\omega}(a)$, $\sigma_0(a)$ that are given in Hahn et al (2008).

Eqn. (9) is the *differential* acceleration that adjacent and opposing streamlines exert on a ring particle due to pressure. Thus this equation does not apply to the ring's outermost streamline, where pressure is due to a single adjacent streamline. To calculate the pressure drop at the outermost streamline, use the *linear momentum flux* $G_p = c^2\sigma$, which is the force-per-length that a streamline exerts on its neighbor. It can then be shown that the particle's acceleration due to the pressure drop at the ring's edge is

$$a_p(a,\theta) = \frac{G_p}{\sigma_0\Delta a} \simeq A_{pr}^0 + A_{pr}^m e^{im(\theta-\theta_s)}, \qquad (10)$$

where Δa is the streamline's semimajor axis width (Hahn et al 2008).

ring viscosity: Viscosity in a planetary ring is due to collisions among particles (Goldreich & Tremaine 1982) or perhaps due to self-gravitating wakes (Daisaka et al 2001). A ring particle's radial and tangential accelerations due to viscous friction are

$$a_{\nu r} \simeq \frac{1}{\sigma}\frac{\partial}{\partial r}\left[\left(\frac{4}{3}\nu_s + \nu_b\right)\sigma\frac{\partial\upsilon_r}{\partial r}\right] \quad \text{and} \quad a_{\nu\theta} \simeq \frac{1}{\sigma}\frac{\partial}{\partial r}\left(\nu_s\sigma r\frac{\partial\upsilon_\theta}{\partial r}\right) \qquad (11)$$

where ν_s and ν_b are the ring's kinematic shear and bulk viscosities (from Landau & Lifshitz 1987). Again, these formulas only apply in the ring's interior, since they are the difference in the accelerations exerted by adjacent and opposing streamlines. To get the acceleration at the outermost streamline, use the viscous linear momentum flux $G_\nu \simeq -\left(\frac{4}{3}\nu_s + \nu_b\right)\sigma(\partial\upsilon_r/\partial r)$ to calculate $a_{\nu r} = G_\nu/\sigma_0\Delta a$. Another useful quantity is the viscous angular momentum flux $F_\nu \simeq 2\nu_s\sigma_0 a\Omega(1/J - 1/4J^2)$ (from Borderies et al 1982), which also provides the tangential viscous acceleration at the ring's edge, $a_{\nu\theta} = F_\nu/\sigma_0 a\Delta a$ (Hahn et al 2008).

torque balance at the ring's outer edge: The ring's outer edge is the site where the viscous torque precisely balances the satellite's torque on the ring. The viscous torque is $\mathcal{L}_\nu = \oint F_\nu d\ell = 3\pi\nu_s\sigma_0 a^2\Omega(1 - \frac{4}{3}q^2)/(1-q^2)^{3/2}$, which is also known as the ring's viscous angular momentum luminosity (AML) (Borderies et al 1982). The torque that the satellite exerts on a single particle is $T_1 = \frac{1}{2}mR_m\Psi_s^m\sin\tilde{\omega}$ (Hahn et al 1995), so the AML due to the satellite's torque is $\mathcal{L}_s(a) = -\int^a T_1 2\pi\sigma_0 a da$, which is the rate at which the satellite withdraws AM from the ring interior to a. The ring's total AML is

$$\mathcal{L}(a) = \mathcal{L}_\nu + \mathcal{L}_s = \frac{3\pi(1-\frac{4}{3}q^2)}{(1-q^2)^{3/2}}\nu_s\sigma_0 a^2\Omega - \int^a m\pi\sigma_0 a R_m\Psi_s^m\sin\tilde{\omega}da, \qquad (12)$$

which must be conserved such that $\mathcal{L}(a) = 3\pi\nu_s\sigma_0 a^2\Omega$ is constant, because static equilibrium requires that the tangential acceleration $A_\theta^0 \propto \partial\mathcal{L}/\partial a = 0$ everywhere in the ring. This supplies a third equation for the third unknown, which is the ring's surface density $\sigma_0(a)$. This equation also tells us where the ring's edge is located, since that must be the site where the AML is purely gravitational, *i.e.*, $\mathcal{L}_s(a_{\rm edge}) = \mathcal{L}$ and $\mathcal{L}_\nu(a_{\rm edge}) = 0$.

numerical solution: The model described by Eqns. (6)–(12) are coupled, nonlinear integro-differential equations. Those equations are solved by representing the ring as N discrete streamlines, replacing integrals with sums, and using finite difference methods to evaluate derivatives. This results in a nonlinear system of $3N$ coupled equations for the N streamlines' e_i, $\tilde{\omega}_i$, and σ_i that are straightforward to solve numerically.

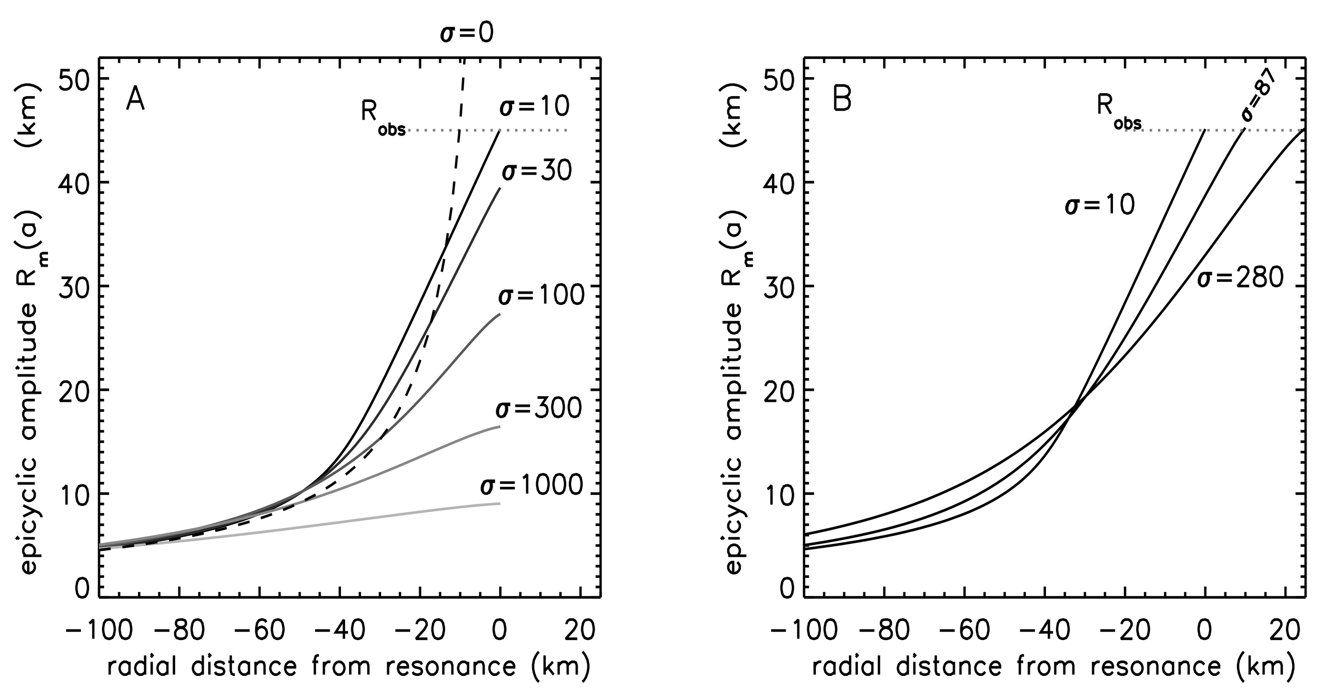

FIGURE 1: Fig. 1A plots the model B ring's epicyclic amplitude R_m versus semimajor axis distance from the resonance, for a variety of rings whose surface densities are indicated in units of gm/cm^2. The dotted line is the B ring's observed epicyclic amplitude, $R_m \simeq 45$ km (Spitale & Porco 2006). Models also show that R_m increases as the ring-edge's distance from resonance is increased, but that can be offset by increasing in the ring's density σ such that $R_m = R_{\rm obs}$; see Fig. 1B.

Model B ring results

Figure 1A show how the ring-edge's epicyclic amplitude $R_m(a)$ depends on the ring's surface density σ; that figure demonstrates that a heavier ring has a smaller R_m. Those models also show that R_m is sensitive to the location the ring's outer edge, with R_m getting larger when its edge lies further beyond resonance. However that increase in R_m can also be offset by increasing the ring's density σ; see Fig. 1B. Also recall that Voyager observations showed that the B ring's outer edge could lie as far as 24 km beyond Mimas $m = 2$ ILR (Porco et al 1984). Fig. 1B thus indicates that the outer B ring's surface density is $10 \lesssim \sigma \lesssim 280$ gm/cm^2. A more rigorous comparison of this model to Cassini measurements of the ring-edge's location should allow us to pin down the ring's σ with greater certainty.

Eqn. (7) also predicts that a perturbed ring should experience significant variations is its surface density, which is plotted in Fig. 2A. Note that the ring-edge's surface density is enhanced $\sim 50\%$ at periapse, due to the satellite's perturbations having shoved streamlines inwards there and compressing them. Curiously, no such periapse-enhancements have been reported in spacecraft observations of sharp ring-edges. This may be due to I/F saturation, which is the saturation of a ring's surface brightness that occurs when optical depths exceeds ~ 0.3 (Porco et al 2008).

Figure 2B also plots the ring's angular momentum luminosities $\mathcal{L}_\nu$ and $\mathcal{L}_s$. As expected, $\mathcal{L}_\nu \to 0$ and $\mathcal{L}_s \to \mathcal{L}$ at the ring's outer edge, which in this B ring simulation lies 24 km beyond Mimas $m = 2$ ILR.

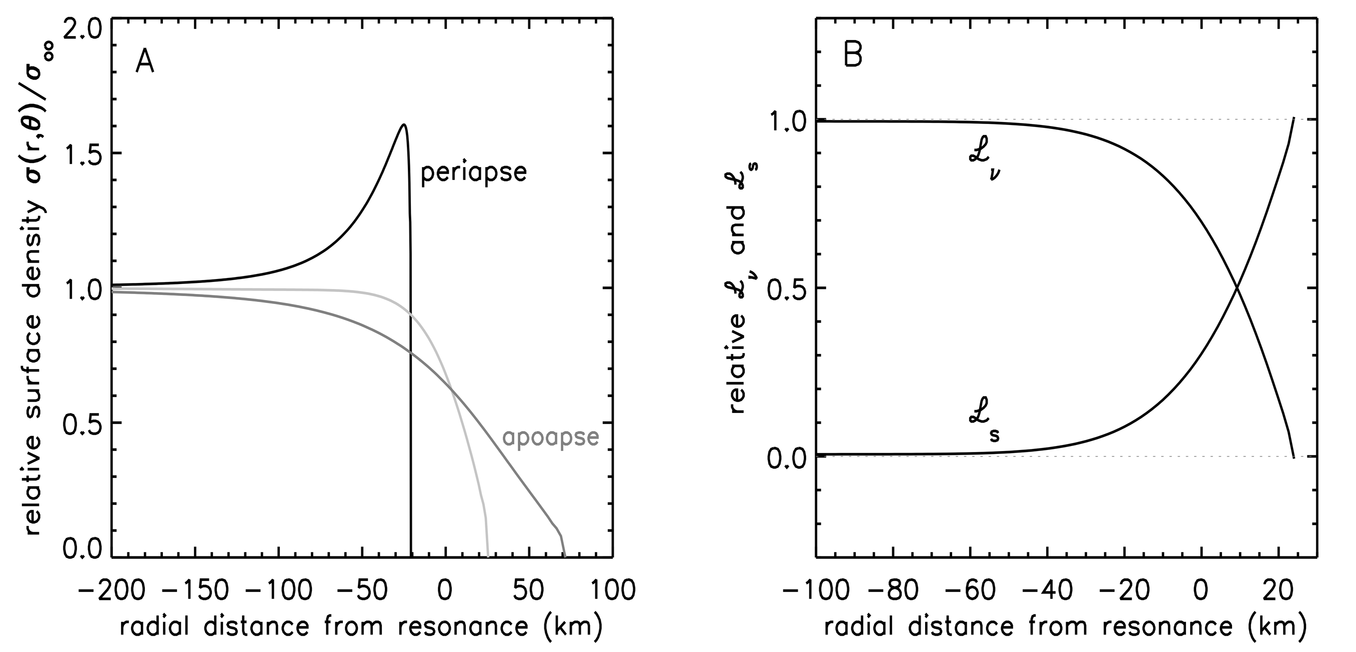

FIGURE 2: Equation (7) is used to calculate relative surface density variations for a model B ring. Figure 2A shows σ versus radius r plotted along three different longitudes: towards the ring's longitude of periapse, its apoapse, and along an intermediate longitude. Figure 2B plots the ring's viscous angular momentum luminosity $\mathcal{L}_\nu$, as well as the AML due to the satellite's torque, $\mathcal{L}_s$, in units of the total $\mathcal{L}$. As expected, $\mathcal{L}_\nu \to 0$ and $\mathcal{L}_s \to \mathcal{L}$ at the ring's outer edge, which lies 24 km beyond Mimas $m = 2$ ILR.

Additional conclusions

- Ring self gravity is the dominant internal ring force. Pressure is weak and unimportant everywhere except at the ring's edge, similar to narrow eccentric ringlets (Chiang & Goldreich 2000, Mosqueira & Estrada 2002).

- The torque that the satellite exerts on a viscous ring is *extremely* weak, smaller than the Goldreich-Tremaine (1978) torque formula by orders of magnitude. This makes balancing the viscous and gravitational torques at the ring edge very difficult. Note that the viscous torque is $\propto \nu_s$ while the satellite's torque $\propto (\nu_s + \nu_b)$. We find that a torque balance is possible when the bulk/shear viscosity ratio is $\nu_b/\nu_s \sim 10^4$. However, it is unclear whether a planetary ring's viscosity can actually satisfy this extreme requirement.

- However, a drag force is *very* effective at enabling the satellite's torque on the ring, as well as maintaining a torque balance at the ring's outer edge. This is due to the larger $|\tilde{\omega}|$ that results from drag (see Eqn. 12).

future activities:
The streamline model developed here is very general, and can be adapted to study narrow eccentric ringlets, and nonlinear spiral density waves. Adapting the model to investigate the A ring's interaction with the coorbital satellites Janus and Epimetheus is also underway (Spitale et al 2008).

acknowledgments:
JMH is supported by NASA's Outer Planets Research Program.

References

Borderies, Goldreich, & Tremaine, 1982, Nature, 299, 209
Borderies, Goldreich, & Tremaine, 1985, Icarus, 63, 406
Chiang & Goldreich, 2000, ApJ, 540, 1084
Daisaka, Tanaka, & Ida, 2001, Icarus, 154, 296
Goldreich & Tremaine, 1978, Icarus, 34, 730
Goldreich & Tremaine, 1982, ARA&A, 20, 249
Hahn, Spitale, & Porco, 2008, in preparation
Hahn, Ward, & Rettig, 1995, Icarus, 117, 25
Landau & Lifshitz, 1987, Fluid Mechanics
Mosqueira & Estrada, 2002, Icarus, 158, 545
Porco et al, 1984, Icarus, 60, 17
Porco et al, 2008, AJ, in press
Spitale & Porco, 2006, LPSC abstract #2242
Spitale et al, 2008, in preparation